

STOCHASTIC MODEL FOR EVALUATING THE PRECISION LANDING OF REENTRY VEHICLE

Teodor-Viorel CHELARU¹, Adrian CHELARU²

The paper presents a random calculus model for calculating the precision of guided flight during terminal phase and automatic landing of a reentry vehicle. The proposed method is based on canonical decomposition of the random inputs, which allows us to obtain directly the output dispersion of the coordinates of the vehicle from the dispersion of any kind of random input signal, which passes through the differential equations of motions by using a decomposition of input signal on pulsation domains (PD) and by integrating the differential equation system for each PD. The novelty of the paper results from the theoretical method of random functions theory, applied to solve the technical problem of precision for guided flight during terminal phase and automatic landing of a reentry vehicle.

Keywords: reentry vehicle, guidance precision, landing, stochastic model, random functions.

Nomenclature

α - Attack angle (tangent definition); β - Sideslip angle (tangent definition); δ_a - Aileron deflection; δ_e - Elevator deflection; δ_r - Rudder deflection; ψ - Azimuth angle; θ - Inclination angle; ϕ - Bank angle; ρ - Air density; Ω - Body angular velocity; A, B, C, E - Inertia moments; $C_x^A; C_y^A; C_z^A$ - Aerodynamic coefficients of force in the body frame; $C_l^A; C_m^A; C_n^A$ - Aerodynamic coefficients of momentum ; $C_x^T; C_y^T; C_z^T$ - Thrust coefficients in the mobile frame; $C_l^T; C_m^T; C_n^T$ - Thrust momentum coefficients in the mobile frame; $F_0 = 0.5\rho V^2 S$ - Reference aerodynamic force; $H_0 = F_0 l$ - Reference aerodynamic couple; T_0 - Reference thrust force; $U_0 = T_0 l$ -Reference couple thrust; l - Reference length; m - Mass; p, q, r - Angular velocity components along the axes of body frame; S - Reference area; t - Time; \mathbf{V} - Velocity vector; u, v, w - Velocity components in body frame; V_x, V_y, V_z -Velocity components in local frame; $OX_0Y_0Z_0$ - Normal

¹ Prof., Faculty of Aerospace Engineering , University POLITEHNICA of Bucharest, Romania, e-mail: teodor.chelaru@upb.ro

² Eng., INCAS -National Institute for Aerospace Research “Elie Carafoli”, Romania, e-mail: chelaru.adrian@incas.ro

local-fixed frame (inertial frame); $Oxyz$ – Body frame (mobile frame); $x_0y_0z_0$ - Coordinates in local-fixed frame . $OX_gY_gZ_g$ - Ground fixed frame (inertial frame);

1. Introduction

One of the current areas of development in the field of space programs is the reentry vehicle. These vehicles are intended to achieve different space missions, from transport of human crew to the space station, till interventions on the orbiting satellites. After the success of the US space shuttle program, the major space agencies are considering the development of reentry vehicles, mostly without crew, which performs automatic flight. At European level, European Space Agency intends that starting from IXV (**I**ntermediate **e**Xperimental **V**ehicle) vehicle, which is a parachuting re-entry vehicle, to achieve a fully automatic re-entry vehicle, PRIDE (**P**rogramme for the **R**eusable **I**n-orbit **D**emonstrator for **E**urope), which will have a guided landing phase [9]. For these types of vehicles there are many problems of study, starting with aerothermodynamic issues specific to high speed, heat transfer, accuracy of guidance, and others, each of them can be the subject of separate studies. This paper is proposing to address one of these issues, namely the one of precision landing, when vehicle velocity is low and we can use usual aerodynamic theory for ordinary aircrafts. To address this, the paper proposes the determination of the landing dispersion zone by developing a stochastic model in which the random input values are the flight parameters measured by the sensors, while the output is represented by the values that describe the vehicle states (velocity, position).

For solving this, there are two possibilities. One of them, developed in work [3], consists in the introduction of certain random input in the system that will simulate, in the context of classic hypothesis, the noises of the signals introduced by the sensors. The determination of the landing dispersion is achieved by building a beam of possibilities for the evolution of the vehicle, in so call “Monte Carlo” methods. Unfortunately, this method, due to finite number of realizable possibilities, gives only a roughly result.

Another method consists in the canonical decomposition of the random functions. This method was founded in paper [1] and developed in papers [2] and [5]. The method separates the problem of vehicle dynamic into two sub-problems: one consisting in the determination of average evolution, which is a deterministic problem, and the second, to obtain the states dispersion. The second problem can be solved through the integration of the supplementary equations obtained from the canonical separation of random terms from the dynamic equations. This method leads to a better quantitative appreciation of the landing dispersion in the case of guided vehicle. Next, in the paper we try to apply the method of canonical

separation for evaluating the precision automatic landing for a reentry vehicle (Fig. 1).

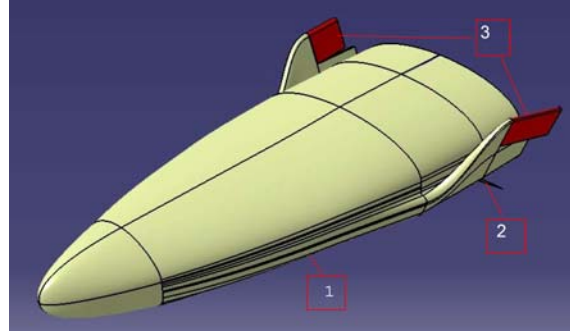


Fig. 1. The reentry vehicle general view (1-body; 2-flaps; 3 – rudders)

2. Equations of Motion

2.1. General Motion Equations for Reentry Vehicle

As shown in the paper [3] the vehicle's dynamic equations are the translation equations, which are achieved from the impulse theorem and the rotation equations, which come from the kinetic moment theorem.

The translation equation can be written in local frame which is an inertial frame as:

$$\dot{\mathbf{V}}_0 = \mathbf{B}_I m^{-1} (F_0 \mathbf{C}_F + T_0 \mathbf{C}_T) + \mathbf{g}_0. \quad (1)$$

where:

$$\mathbf{C}_F = [C_x^A \quad C_y^A \quad C_z^A]^T; \quad \mathbf{C}_T = [C_x^T \quad C_y^T \quad C_z^T]^T \quad (2)$$

are the aerodynamic coefficients and trust coefficients in body frame, and the matrix \mathbf{B}_I is defined using the Euler's angles:

$$\mathbf{B}_I = \begin{bmatrix} \cos \psi \cos \theta & -\sin \psi \cos \phi + \cos \psi \sin \theta \sin \phi & \sin \psi \sin \phi + \cos \psi \sin \theta \cos \phi \\ -\sin \psi \cos \theta & -\cos \psi \cos \phi - \sin \psi \sin \theta \sin \phi & \cos \psi \sin \phi - \sin \psi \sin \theta \cos \phi \\ \sin \theta & -\cos \theta \sin \phi & -\cos \theta \cos \phi \end{bmatrix} \quad (3)$$

The rotation equation around the center of the mass, written in the body frame is:

$$\dot{\mathbf{\Omega}} = \mathbf{J}^{-1} (H_0 \mathbf{C}_H + U_0 \mathbf{C}_U) + \mathbf{J}^{-1} \mathbf{A}_\Omega \mathbf{J} \mathbf{\Omega}, \quad (4)$$

where:

$$\mathbf{C}_H = [C_l^A \quad C_m^A \quad C_n^A]^T; \quad \mathbf{C}_U = [C_l^T \quad C_m^T \quad C_n^T]^T \quad (5)$$

are aerodynamic and thrust moment coefficients in body frame, and \mathbf{J}^{-1} is the inverse matrix for the inertia moment .

The kinematical equations are additional equations, which allow us to obtain the linear coordinates in local frame:

$$[\dot{x}_0 \quad \dot{y}_0 \quad \dot{z}_0]^T = [V_x \quad V_y \quad V_z]^T. \quad (6)$$

For Euler's angle when the angular velocity components are known we have:

$$[\dot{\phi} \quad \dot{\theta} \quad \dot{\psi}]^T = \mathbf{W}_A [p \quad q \quad r]^T, \quad (7)$$

where:

$$\mathbf{W}_A = \begin{bmatrix} 1 & \sin \phi \operatorname{tg} \theta & \cos \phi \operatorname{tg} \theta \\ 0 & \cos \phi & -\sin \phi \\ 0 & \sin \phi \sec \theta & \cos \phi \sec \theta \end{bmatrix}, \quad (8)$$

2.2. Guidance Command

Resuming [3], the guidance commands for vehicle flight are:

$$\begin{aligned} u_a &= -u_\phi + u_\psi \sin \theta; \\ u_e &= u_{eb} + u_y (\sin \phi \cos \psi - \cos \phi \sin \theta \sin \psi) - u_z \cos \phi \cos \theta - u_\theta \cos \phi - u_\psi \sin \phi \cos \theta; \\ u_r &= u_y (\cos \phi \cos \psi + \sin \phi \sin \theta \sin \psi) + u_z \sin \phi \cos \theta + u_\theta \sin \phi - u_\psi \cos \phi \cos \theta; \\ u_T &= u_{Tb} - k_u^u \tilde{u}. \end{aligned} \quad (9)$$

where, angular signal command are u_ϕ - Roll command; u_θ - Pitch command; u_ψ - Yaw command, u_y, u_z - Linear command; u_T - Thrust command;
Roll command assure roll control by following imposed yaw angle:

$$u_\phi = k_u^\phi \dot{\phi} + k_u^{\dot{\phi}} \dot{\phi} - k_u^{\psi*} \tilde{\psi} \cos \theta. \quad (10)$$

Pitch command assures longitudinal attitude control:

$$u_\theta = k_u^\theta \tilde{\theta} + k_u^{\dot{\theta}} \dot{\tilde{\theta}} + k_u^I I_\theta, \quad (11)$$

and Yaw command assure heading control:

$$u_\psi = k_u^\psi \tilde{\psi} + k_u^{\dot{\psi}} \dot{\tilde{\psi}}, \quad (12)$$

Linear command terms are:

$$u_y = k_u^{\lambda_y} \lambda_y + k_u^{h_y} h_y; \quad u_z = k_u^{\lambda_z} \lambda_z + k_u^{h_z} h_z \quad (13)$$

The guidance commands are applied through the actuators which are approximated in the paper [3] by relations:

$$\begin{aligned} \dot{\delta}_T &= -\frac{\delta_T}{\tau_{\delta T}} + \frac{k_{\delta T}^u u_T}{\tau_{\delta T}}; \quad \dot{\delta}_a = -\frac{\delta_a}{\tau_{\delta a}} + \frac{k_{\delta a}^u u_a}{\tau_{\delta a}}; \\ \dot{\delta}_e &= -\frac{\delta_e}{\tau_{\delta e}} + \frac{k_{\delta e}^u u_e}{\tau_{\delta e}}; \quad \dot{\delta}_r = -\frac{\delta_r}{\tau_{\delta r}} + \frac{k_{\delta r}^u u_r}{\tau_{\delta r}} \end{aligned} \quad (14)$$

where $\tau_{\delta T}; \tau_{\delta \alpha}; \tau_{\delta \dot{\alpha}}; \tau_{\delta \dot{\theta}}$ are the time constants and $k_{\delta T}^u; k_{\delta \alpha}^u; k_{\delta \dot{\alpha}}^u; k_{\delta \dot{\theta}}^u$ are the gain constants.

Also, we use integral term, defined as:

$$\dot{I}_\theta = \tilde{\theta}. \quad (15)$$

2.3. Particularities Equation of Motion for Symmetrical Evolution

Next, starting from dynamic translation equations rewritten in quasi-velocity frame [3] we will analyse the particular case of a symmetric evolution, which ensure the separation of the longitudinal equation of motion by lateral equation of motion and finally allow convenient linearization of the motion equation.

For consistence of lateral motion equation, specific parameters of this motion will be considerate small, but different from zero. Based on these approximations, we can evaluate for the beginning the expression of aerodynamics angles, obtaining:

$$\gamma = \theta - \alpha. \quad (16)$$

respectively:

$$\beta \cos \alpha = (\psi - \chi) \cos \gamma - \phi \sin \alpha. \quad (17)$$

Doing as in paper [3], if we consider the flight in a vertical plane and we neglect the influences of the small terms, from (7) we obtain:

$$\dot{\phi} = p + r \operatorname{tg} \theta + q \phi \operatorname{tg} \theta; \quad \dot{\theta} = q; \quad \dot{\psi} = r \sec \theta + q \phi \sec \theta \quad (18)$$

In this case, as shown in the same paper [3], we can separate the longitudinal and lateral motion. Hence, the lateral equations of motion are written in the following form:

$$\begin{aligned} \dot{\beta} &= r - \frac{F_0 C_y}{mu} - p \operatorname{tg} \alpha - \frac{\phi}{u} g \cos \theta; \\ \dot{r} &= \frac{H_0}{C} C_n^A + \frac{U_0}{C} C_n^T + \frac{E}{CA} (H_0 C_l^A + U_0 C_l^T) + \frac{A-B}{C} pq - \frac{E}{C} qr; \\ \dot{p} &= \frac{H_0}{A} C_l^A + \frac{U_0}{A} C_l^T + \frac{E}{CA} (H_0 C_n^A + U_0 C_n^T) + \frac{B-C}{A} qr + \frac{E}{C} pq; \\ \dot{\phi} &= p + r \operatorname{tg} \theta + q \phi \operatorname{tg} \theta; \quad \dot{\psi} = r \sec \theta + q \phi \sec \theta; \\ \dot{y}_0 &= V(\beta \cos \alpha - \psi \cos \gamma + \phi \sin \alpha), \end{aligned} \quad (19)$$

to which we add the relation (17).

These equations represent the lateral decoupled equations of motion written in the specific case of the vehicle evolution in vertical plane.

3. The linearized form of equation of motion

3.1. Linear Form of Lateral Equation

The equations (19), presented in the previous section can be linearized and together with (17) obtaining:

$$\begin{aligned}
 \Delta\dot{\beta} &= a_{\beta}^{\beta}\Delta\beta + a_r^r\Delta r + a_p^p\Delta p + a_{\beta}^{\phi}\Delta\phi + a_{\beta}^{\dot{\beta}}\Delta\dot{\beta} + b_{\beta}^{\delta r}\Delta\delta_r + b_{\beta}^{\delta a}\Delta\delta_a + \\
 &+ a_{\beta}^{\beta_w}\Delta\beta_w + \Delta Y_p^* / (mu) \\
 \Delta\dot{r} &= a_r^{\beta}\Delta\beta + a_r^r\Delta r + a_p^p\Delta p + a_p^{\dot{\beta}}\Delta\dot{\beta} + b_r^{\delta r}\Delta\delta_r + b_r^{\delta a}\Delta\delta_a + a_r^{\beta_w}\Delta\beta_w + \Delta N_p^* / C \quad (20) \\
 \Delta\dot{p} &= a_p^{\beta}\Delta\beta + a_p^p\Delta p + a_p^r\Delta r + a_p^{\dot{\beta}}\Delta\dot{\beta} + b_p^{\delta r}\Delta\delta_r + b_p^{\delta a}\Delta\delta_a + a_p^{\beta_w}\Delta\beta_w + \Delta L_p^* / A \\
 \Delta\dot{\phi} &= a_{\phi}^r\Delta r + \Delta p + a_{\phi}^{\phi}\Delta\phi; \Delta\psi = a_{\psi}^r\Delta r + a_{\psi}^{\phi}\Delta\phi; \Delta\dot{y}_0 = a_y^{\beta}\Delta\beta + a_y^{\phi}\Delta\phi + a_y^{\psi}\Delta\psi.
 \end{aligned}$$

where : β_w - Wind sideslip angle (Cross win influence); Y_p^* - Lateral perturbation force except wind influence; $L_p^* N_p^*$ - Perturbation roll and yaw moments except wind influence; All the coefficients are described in work [3].

From relation (20) we can obtain immediately the stability matrix and the command matrix for lateral motion of vehicle.

3.2. Lateral Extended Stability, Command and Control Matrices

Besides the general motion equations in linear form as outlined above, flight vehicle needs other relationships to be added. Among them, the most important and which can not be neglected are the actuator equations and the guidance equations. For the autonomous flight, as is case of a reentry vehicle, the guidance equation is necessary to introduce integrated terms specific to PID (Proportional-Integrative – Derivative) -type controllers.

Starting from (14) linear form of the actuator equation for lateral motion becomes:

$$\Delta\dot{\delta}_e = -\frac{\Delta\delta_e}{\tau_{\delta_e}} + \frac{k_{\delta_e}^u\Delta u_e}{\tau_{\delta_e}}; \quad \Delta\dot{\delta}_r = -\frac{\Delta\delta_r}{\tau_{\delta_r}} + \frac{k_{\delta_r}^u\Delta u_r}{\tau_{\delta_r}} \quad (21)$$

Using linear relation (20) and (21) we can build extended stability and command matrices indicated in paper [5]. Also, by linearizing the relation (9) for lateral commands we obtain control matrix:

Table 1

Lateral control matrix (controller) **K**

		1	2	3	4	5	6	7	8
		β	r	p	ϕ	ψ	y_0	δ_a	δ_r
1	u_a		k_{ua}^r	k_{ua}^p	k_{ua}^{ϕ}	k_{ua}^{ψ}			
2	u_r	k_{ur}^{β}	k_{ur}^r		k_{ur}^{ϕ}	k_{ur}^{ψ}	k_{ur}^y		

where:

$$\begin{aligned} k_{ua}^r &= -k_{\delta}^r \sin \theta ; k_{ua}^p = k_{\delta}^p ; k_{ua}^{\phi} = k_{\delta}^{\phi} ; k_{ua}^{\psi} = -(k_{\delta}^{\psi} \sin \theta + k_{\delta}^{\psi*} \cos \theta) ; \\ k_{ur}^{\beta} &= -k_{\delta}^{\lambda} V \cos \alpha ; k_{ur}^r = k_{\delta}^r \cos \theta ; k_{ur}^{\phi} = -k_{\delta}^{\lambda} V \sin \alpha ; k_{ur}^{\psi} = k_{\delta}^{\lambda} V \cos \gamma + k_{\delta}^{\psi} \cos \theta ; \\ k_{ur}^y &= -k_{\delta}^h . \end{aligned}$$

In this case, we have the system that describes lateral controlled motion in form:

$$\dot{\mathbf{x}} = \mathbf{Ax} + \mathbf{Bu} ; \mathbf{u} = -\mathbf{Kx} \quad (22)$$

where:

$$\mathbf{A} = [\mathbf{I} - \mathbf{A}_1]^{-1} \mathbf{A}_0 \quad \mathbf{B} = [\mathbf{I} - \mathbf{A}_1]^{-1} \mathbf{B}_0$$

The stability and command matrices $\mathbf{A}_0, \mathbf{A}_1, \mathbf{B}_0$ are indicated in paper [5]

4. Canonical decomposition method

In the following, we present a numerical method, based on canonical decomposition of the random variables to solve this class of problems, which can be easily implemented in calculus software. The method consists of integrating the equations (22) using the canonical decomposition of random functions, according to the method presented in work [1].

This method allows obtaining the output signal dispersion from the input signal dispersion for any kind of differential linear unsteady equations. For that, we use a decomposition of input signal in a number of pulsation domains (PD) and integrate differential equation system for each of them.

The method is an approximation, because the number of PD is limited. Theoretically, if we use an infinite number of PD we can obtain the exact solutions. To evaluate the accuracy of the method firstly we analyse a simple case, like a test case, with known analytical solutions.

4.1 Calculus Example, Dispersion Evaluation

Therefore, we choose, as example, the well known linear stationary equation with constant coefficients:

$$dy/dt = -y/\tau_1 + x/\tau_1 . \quad (23)$$

After the Laplace transformation, the equation can be put as a transfer function:

$$y = \frac{1}{\tau_1 s + 1} x . \quad (24)$$

Considering as input random variable x , similarly with “white noise”³, centred in zero, to output will be a random signal y also centred in zero. The analytical link between spectral densities of the signals is given by:

$$S_y = \left| \frac{1}{\tau_1 i \omega + 1} \right|^2 S_x = \frac{1}{\tau_1^2 \omega^2 + 1} S_x, \quad (25)$$

The dispersion of the output signal can be obtained through integration of the spectral density related to the pulsation ω :

$$D_y = 2 \int_0^\infty S_y d\omega = \lim_{\omega \rightarrow \infty} \frac{2S_x}{\tau_1} \arctan \tau_1 \omega = \frac{\pi S_x}{\tau_1}, \quad (26)$$

where it was taken in the consideration that spectral density of the input signal does not depend by pulsation. As numerical example we took the time constant $\tau_1 = 0,5 [s]$, and as input the signal $S_x = 0,00394 [s]$ with dispersion $D_x = 1$ for a maximum pulsation $\omega_{\max} = 127 [1/s]$. Using the analytical relation (26) we obtained $D_{y4} = 0,02468$

For the calculus example, we noticed that the PD for the spectral density of the output signal is limited, transfer function (24) working as a “low band” filter (cut the high frequencies). In this case, in our example we could approximate the spectral density of the input signal with a rectangle, which contains PD in which the output spectral density has values.

In work[1] it is shown that for an unsteady random function $x(t)$ it can be used a canonical decomposition:

$$x(t) = m_x(t) + \overset{\circ}{x}(t) = m_x(t) + \sum_{k=1}^n V_k \varphi_k(t), \quad (27)$$

where: $\overset{\circ}{x}(t)$ is a centred unsteady function; $m_x(t)$ is an average function, V_k are the random quantities and $\varphi_k(t)$ are the coordinate deterministic functions. Also, in this work it is shown the link between coordinate functions of the input separated signal and the output separated signal. This link allows building the spectral density and dispersion of the output signal using spectral density of the input signal. If the input signal is stationary, the coordinate functions have a particular form: $\varphi_k(t) = e^{i\omega_k t}$. In this case, supposing that the input signal is stationary and centred we can use the following decomposition:

$$\overset{\circ}{x} = \sum_{\substack{k=-n \\ k \neq 0}}^n W_k e^{i\omega_k t}, \quad (28)$$

³ Different from “white noise”, the input used is defined over a finite frequencies domain.

where W_k it is complex random centred quantity with the dispersion $D_k = 2D_K^* = 2D[W_k]$ obtained from the spectral density for the input signal $S_x(\omega_k) = 2S_x^*(\omega_k)$ corresponding a pulsation band $\Delta\omega_k$ centred in pulsation ω_k . Because input signal is even, we can write:

$$D_x = \sum_{\substack{k=-n \\ k \neq 0}}^n D_k^* = \sum_{k=1}^n D_k. \quad (29)$$

If the coordinate functions for the input signal are $\varphi_k(t) = e^{j\omega_k t}$, and the coordinate functions for output signal are $\psi_k(t)$, the dispersion for the output signal can be obtained with relation:

$$D_y(t) = 2 \sum_{k=1}^n D_k |\psi_k(t)|^2, \quad (30)$$

where coordinate functions of the output signal can be obtained from coordinate functions of the input signal through equation (23). We can build an equation system, containing an equation for each pulsation ω_k :

$$\psi_k(t) = -\psi_k(t)/\tau + \varphi_k(t)/\tau, \quad (31)$$

where: $k = 1 \dots n$.

Because the functions $\varphi_k(t), \psi_k(t)$, are complex, the solution of the system (31) can be obtained by separating the imaginary part from real part:

$$\dot{y}_{1k}(t) = -y_{1k}(t)/\tau + \cos(\omega_k t)/\tau; \quad \dot{y}_{2k}(t) = -y_{2k}(t)/\tau + \sin(\omega_k t)/\tau, \quad (32)$$

where: $y_{1k} = \text{Re } \psi_k(t)$; $y_{2k} = \text{Im } \psi_k(t)$, and $k = 1 \dots n$.

Together with the system solution we obtained the square of the coordinate function corresponding the pulsation ω_k : $\psi_k^2 = y_{1k}^2 + y_{2k}^2$, and also the dispersion corresponding to the pulsation band $\Delta\omega_k$: $D_k = S_x \Delta\omega_k$. Using relation (30) until maximum pulsation $\omega_{\max} = 127$, for a pulsation number $n = 500$ and time $t_{\max} = 5$ we obtained the output signal dispersion, which for numerical application has the value $D_{yN} = 0,02443$. For this application, we directly evaluated the relative error between analytical result and numerical result:

$$\Delta\% = \frac{D_{yA} - D_{yN}}{D_{yA}} \cdot 100 = \frac{0.002468 - 0.02443}{0.002468} \cdot 100 \approx 1\% \quad (33)$$

4.2 Dispersion of Flight Parameters for reentry vehicle

For the re-entry vehicle case, we can put linear system (22) in a form similarly with (23):

$$dY/dt = \mathbf{A}Y - \mathbf{B}KX, \quad (34)$$

where X is a random input signal and Y is a random output signal. Because the system describes an autonomous motion where states Y follows reference values Y_D , the input and output signals can be considered in form:

$$X = Y - Y_D + \dot{X}, \quad Y = \bar{Y} + \dot{Y} \quad (35)$$

where \dot{X} is a noise introduced by sensors that measure the system states. The \bar{Y} means the average of random states variables and \dot{Y} is output unsteady random centred signal. \mathbf{D} matrix allows us to choose the sensors that introduce the noise. In this case, the equation (34) can be separate in two equations. First is a deterministic one, in average of states:

$$d\bar{Y}/dt = (\mathbf{A} - \mathbf{B}\mathbf{K})\bar{Y} + \mathbf{B}\mathbf{K}Y_D, \quad (36)$$

and the second an equation in random variables:

$$d\dot{Y}/dt = (\mathbf{A} - \mathbf{B}\mathbf{K})\dot{Y} - \mathbf{B}\mathbf{K}\dot{X}, \quad (37)$$

The solution \dot{Y} of equation (37) means getting the dispersion of the system state when we know the dispersion of the input X , namely the dispersion of the signal measured by sensors. In order to obtain the solutions we proceed similarly to previous calculus example, by building an equations system in coordinate functions and separate the real part from the imaginary part for each equation:

$$\begin{aligned} \dot{y}_{Rik}(t) &= (a_i^j - b_i^j k_i^j) y_{Rjk}(t) - b_i^j k_i^j \delta_j \cos(\omega_k t), \\ \dot{y}_{lik}(t) &= (a_i^j - b_i^j k_i^j) y_{ljk}(t) - b_i^j k_i^j \delta_j \sin(\omega_k t) \end{aligned} \quad (38)$$

where:

$$\delta_j = \begin{cases} = 1 & \text{if sensor j is working} \\ = 0 & \text{if sensor j is not working} \end{cases}.$$

Taking into account the number of the states (8) the number of frequencies (200) and the fact that each equation must be solved in real and in imaginary parts, finally we have a system of 3200 ordinary differential equations, system which can be solved by numerical methods.

5. Input Data, Results

5.1 Input Data for the Model

Geometrical data

As input data, we use the geometrical elements of the vehicle from figure 2.

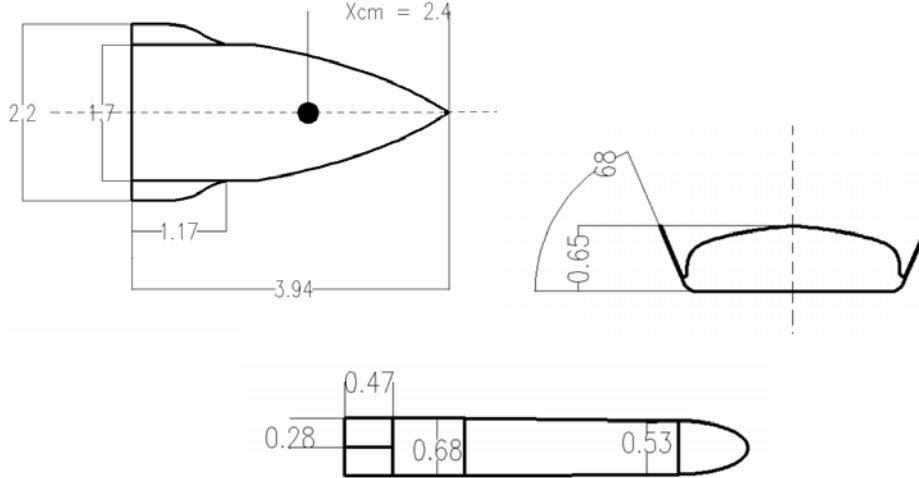


Fig. 2. The reentry vehicle geometry (all dimensions in m)

Geometrical characteristics for the model are: Reference length – body length $l = 3.94 \text{ m}$; Reference area – cross body area $S = 1.131 \text{ m}^2$;

Mechanical data

Mass characteristics of the model are: $m = 1000 \text{ kg}$;

Centre of mass position: $x_{cm} = 2.4 \text{ m}$.

Inertial moments: $A = 512 \text{ kgm}^2$; $B = 827 \text{ kgm}^2$; $C = 1191 \text{ kgm}^2$; $E = 1.4 \text{ kgm}^2$

Aerodynamic data

For the configuration from Fig 2, considering a Taylor series expanding around the origin and by taking into account the parity of the terms, we obtain the following polynomial form of the aerodynamic coefficients in a body frame:

$$\begin{aligned}
 C_x^A &= a_1 + a_{21}\alpha^2 + a_{22}\beta^2 + a_6\delta_e^2 + a_7\delta_a^2 + a_8\delta_r^2 + a_9\alpha + a_{10}\hat{q}\delta_e + a_{13}\alpha^3 + a_{14}\alpha^4 \\
 C_y^A &= b_{12}\beta + b_{42}\hat{r} + b_{52}\delta_r + b_6\delta_a + b_{92}\hat{\beta} + b_{10}\hat{p} \\
 C_z^A &= b_0 + b_{11}\alpha + b_{41}\hat{q} + b_{51}\delta_e + b_{91}\hat{\alpha} + b_{13}\alpha^2 + b_{14}\alpha^3 \\
 C_l^A &= c_3\hat{p} + c_5\hat{r} + c_6\delta_a + c_7\delta_r + c_{13}\beta \\
 C_m^A &= d_0 + d_{11}\alpha + d_{41}\hat{q} + d_{51}\delta_e + d_{91}\hat{\alpha} \\
 C_n^A &= d_{12}\beta + d_{42}\hat{r} + d_{52}\delta_r + d_6\delta_a + d_{92}\hat{\beta} + d_{10}\hat{p} ,
 \end{aligned} \tag{39}$$

where the coefficients $a_1, a_{21} \dots$ generally are depending on Mach number. and, by definition[7]

$$\alpha = -\arctan(v/u), \beta = \arctan(w/u). \tag{40}$$

Stability, command and control matrices

Using aerodynamical and mechanical data we can obtain stability and command derivatives as well as controller parameter. For descending flight with velocity $V = 300 \text{ m/s}$ and climb angle $\gamma = -30^\circ$, at altitude of $H = 1000 \text{ m}$ we obtain the following values:

$$\begin{aligned} a_\beta^\beta &= -0.5; a_\beta^r = 1; a_\beta^p = -0.04; a_\beta^\phi = -0.03; b_\beta^{\dot{\alpha}} = -0.09; b_\beta^{\dot{r}} = 0.09; \\ a_r^\beta &= -24.9; a_r^r = 0.0004; a_r^p = 0.09; b_r^{\dot{\alpha}} = -21.2; b_r^{\dot{r}} = 21.2 \\ a_p^\beta &= 24.7; a_p^r = 0.33; a_p^p = -0.37; b_p^{\dot{\alpha}} = 129.2; b_p^{\dot{r}} = -44.7; \\ a_\phi^r &= -0.31; a_\phi^p = 1.; a_\psi^r = 1.05; a_y^\beta = 300.; a_y^\phi = 12.3; a_y^\psi = -284.5. \tau_{\dot{\alpha}}^{-1} = 10.; \\ \tau_{\dot{r}}^{-1} &= 10.; \end{aligned}$$

After controller synthesis using the gradient modified technique [4] we obtain following optimal values:

$$\begin{aligned} k_{ua}^r &= 0.27; k_{ua}^p = 0.86; k_{ua}^\phi = 2.4; k_{ua}^\psi = -0.17; k_{ur}^\beta = -13.7; k_{ur}^r = 0.84; \\ k_{ur}^\phi &= -0.55; k_{ur}^\psi = 14.7; k_{ur}^y = -0.04. \end{aligned}$$

5.2 Results

Because we have chosen to analyse the lateral motion, as results we will present the influence of the noise of different sensors to the lateral coordinate y . We will consider a constant standard deviation (STD) of the input signal the time evolution of the STD of the lateral coordinate y .

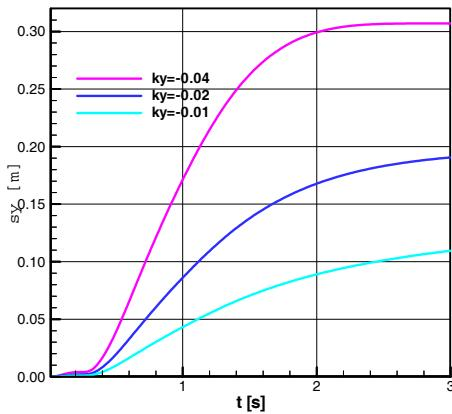


Fig. 3. Influence of the sensor noise by lateral coordinate y_0 on lateral coordinate y_0 .

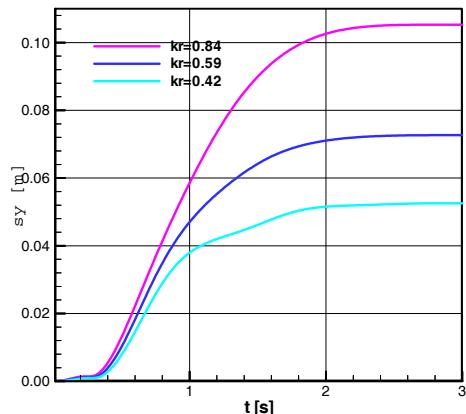


Fig. 4. Influence of the sensor noise by yaw angular velocity r on lateral coordinate y_0 .

Figure 3 presents STD of the lateral position y_0 due by the noise of the y_0 sensor, for different gain values $k_{ur}^y = [-0.04; -0.02; -0.01]$. STD input signal for y sensor is $\sigma = 2.23 \text{ m}$. It can be seen that increasing the gain module values leads to increased lateral deviation.

Figure 4 presents STD of the lateral position y_0 due by the noise of the sensor for angular velocity r for different gain values $k_{ur}^r = [0.84; 0.59; 0.42]$. STD input signal for r sensor is $\sigma = 2.23 \text{ [deg/s]}$. It can be seen that increasing the gain module values leads to decreased lateral deviation.

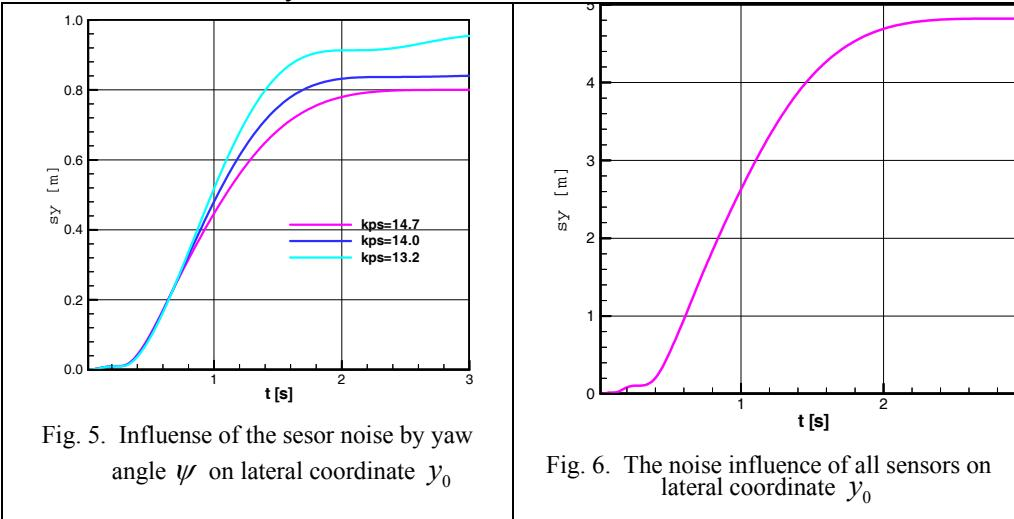
Figure 5 presents STD of the lateral position y_0 due by the noise of the sensor for yaw angle ψ , for different gain values $k_{ur}^\psi = [14.7; 14.0; 13.2]$. STD input signal for ψ sensor is $\sigma = 1 \text{ [deg]}$. It can be seen that increasing the gain module values leads to increased lateral deviation.

Figure 6 shows influence of all sensors on lateral deviation y_0 . In order to obtain this synthetic diagram, we considered:

All angular sizes read by the sensors have STD 1 degree.

All angular velocity sizes read by the sensors have STD 1 degree.

All linear sizes read by sensors have STD 1 m.



6. Conclusions

As we showed in the introduction, for solving problems of accuracy guided flight, such as the automatic landing of reentry vehicle, there are two possibilities: the first one is based on random number generators, leading to methods of the "Monte Carlo" type; the second, based on canonical decomposition of random

variables and integration of equations by coordinated functions. In the sense of the second choices, the paper makes an assessment of the landing precision of the reentry vehicle, by evaluating the lateral deviation due to the noise introduced by the sensors. For this purpose, first we built a calculus linearized model for the vehicle and we determined the stability matrix, command matrix and control matrix. After that, was presented some calculation methods based on the canonical decomposition along with a sample calculation to verify the accuracy of the method. Finally, the calculation method was applied to the system of equations associated with reentry vehicle and we obtained some results concerning the influence of sensor noise on the lateral deviation during landing. Considering preliminary stage of this type of project, with a configuration which is to be defined, the results are not final and may be resumed during the evolution of the project.

What is actually important, and is the novelty of the work, is the proposed method, which is less used in current technical applications, but can even be used to cross check the results with the most popular methods of "Monte Carlo" type.

Acknoledgement

The work has been funded by the Sectoral Operational Programme Human Resources Development 2007 - 2013 of the Ministry of European Funds through the Financial Agreement POSDRU/159/1.5/S/132395.

R E F E R E N C E S

- [1] *E.C. Венцель*, Теория вероятностей (The Theory of Probability), Издательство «Наука», Москва, 1964
- [2] *T.V.Chelaru*, Dinamica zborului – Racheta dirijată - Ed.2 revizuită și adăugită (Dynamnic Flight – The Guided Missile- 2nd Edition Enlarged). Editura Printech. București 2004.
- [3] *T.V.Chelaru*, Dinamica zborului – Racheta dirijată - Ed.2 revizuită și adăugită (Dynamnic Flight – The Guided Missile- 2nd Edition Enlarged). Editura Printech. București 2004.
- [4] *T.V. Chelaru*, Dinamica Zborului – Proiectarea avionului fără pilot (Dynamnic Flight – UAV's design), Ed. Printech, București, ISBN 973-652-751-4, 308 pag, aprilie 2003.
- [5] *T.V. Chelaru, A.Chelaru*, Mathematical Model of Unmanned Aerial Vehicle Used for Endurance Autonomous Monitoring. Proceedings of ICNPAA 2014 - Mathematical Problems in Engineering, Aerospace and Sciences, Narvik, Norway, 15-18 July 2014.
- [6] *T.V. Chelaru, M. Cernat*, Mathematical Calculation Model for Guidance Precision, Target Hit and Target Kill Probability in the Case of Close Range- Homing Missiles, Journal of Battlefield Technology vol. 10, no. 2, pp. 9-14, ISSN 1440-5113 2008 Ed. Argos Press, July 2007, Canberra, Australia.
- [7] *И.Е.Казаков,А.Ф.Мицаков*,Авиационные управляемые ракеты (Aircraft Missiles), Издание ВВИА "Н.Е. ЖУКОВСКОГО",1985.
- [8] *J.N Nielsen*, Missile Aerodynamics, McGraw-Hill Book Company, Inc., New-York, Toronto, London, 1960
- [9] *M. De Stefano Fumo, A. Pugliese, G. Pezzella, G.Giodotti* Small Autonomus Winged Aeroshape Trade-Off through Mission and System Guidelines. 65th International Astronautical Congress, (CD) ISSN 1995-6258, IAC-14-D2.6.5, pp. 1-9, Toronto, Canada, 29 September - 3 October 2014.
- [10] xxx, SLATEC Common Mathematical Library, Version 4.1, July 1993